

Further progress in ion back-flow reduction with patterned gaseous hole - multipliers.

A. V. Lyashenko^{a*}, A. Breskin^a, R. Chechik^a, J. F. C. A. Veloso^b, J. M. F. Dos Santos^c, and F. D. Amaro^c

^a *Department of Particle Physics, Weizmann Institute of Science, 76100, Rehovot, Israel*

^b *University of Aveiro, 3810-193 Aveiro, Portugal*

^c *University of Coimbra, 3004-516 Coimbra, Portugal*

E-mail: alexey.lyashenko@weizmann.ac.il

ABSTRACT: A new idea on electrostatic deviation and capture of back-drifting avalanche-ions in cascaded gaseous hole-multipliers is presented. It involves a flipped reversed-bias Micro-Hole & Strip Plate (F-R-MHSP) element, the strips of which are facing the drift region of the multiplier. The ions, originating from successive multiplication stages, are efficiently deviated and captured by such electrode. Experimental results are provided comparing the ion-blocking capability of the F-R-MHSP to that of the reversed-bias Micro-Hole & Strip Plate (R-MHSP) and the Gas Electron Multiplier (GEM). Best ion-blocking results in cascaded hole-multipliers were reached with a detector having the F-R-MHSP as the first multiplication element. A three-element F-R-MHSP/GEM/MHSP cascaded multiplier operated in atmospheric-pressure Ar/CH₄ (95/5), at total gain of $\sim 10^5$, yielded ion back-flow fractions of $3 \cdot 10^{-4}$ and $1.5 \cdot 10^{-4}$, at drift fields of 0.5 and 0.2 kV/cm, respectively. We describe the F-R-MHSP concept and the relevance of the obtained ion back-flow fractions to various applications; further ideas are also discussed.

KEYWORDS: electron multipliers (gas); avalanche induced secondary effects; charge transport and multiplication in gas; detector modeling and simulations II.

*Corresponding author.

Contents

1. Introduction.	1
2. The F-R-MHSP concept	2
3. Methodology.	2
4. Experimental studies and results.	3
4.1 Single-electron detection efficiency of R-MHSP and F-R-MHSP	3
4.2 Studies of ion blocking capability of the first element in a cascade	9
4.3 IBF in cascaded multipliers incorporating R-MHSP, F-R-MHSP, GEM and MHSP elements.	11
5. General discussion	13

1. Introduction.

In a recent article [1] we summarized the state of the art in avalanche-ion blocking in cascaded gas-avalanche electron multipliers combining GEM and Microhole Hole & Strip (MHSP) [2] elements. The particular cases of Gaseous Photomultipliers (GPM) and Time Projection Chambers (TPC) were discussed in some detail. With some of the techniques discussed in [1], the ion backflow fraction (IBF), namely the fraction of the final-avalanche ions flowing back to the drift volume of a tracking detector, or that impinging on the photocathode (PC) surface of a GPM, could be reduced to values below 10^{-3} in a direct current (DC) operation mode. We discussed the fact that this number is still too large in some applications and that a gated-mode operation, though reducing the IBF down to values below 10^{-4} [3, 4], cannot always be a solution (lack of trigger, dead-time, pick-up noise etc.). The recently proposed and currently investigated ion blocking concept by photon-assisted avalanche propagation in cascaded multipliers [5, 6] has some interesting aspects. However, it is limited to an operation with highly scintillating gas mixtures, in the far UV; furthermore, methods have to be conceived for blocking the ions originating from the avalanche developing in the first multiplication/scintillation element of the cascaded detector.

Some of the ideas and results published in [1, 7, 8] suggested ion blocking with a reversed-bias Micro-Hole & Strip Plate (R-MHSP) used as a first element in a multipliers' cascade. This method, in which ions are deviated and neutralized on strip-electrodes patterned on the surface of a hole-multiplier figure 1, provided a good suppression of ions flowing back from successive elements into the R-MHSP. However, a large fraction of ions originated from avalanches occurring within the R-MHSP holes remained unblocked. Therefore, another DC ion-blocking method have been recently conceived and evaluated, aiming at more efficient electrostatic deviation of the drifting ions towards collecting strip-electrodes patterned at the holes vicinity.

The present work describes the new concept of "Flipped" Reversed-bias Micro-Hole & Strip Plate (F-R-MHSP) electrodes in which strips are pointing up towards the drift region of the multiplier. Simulation and experimental results of electron collection and ion blocking of the F-R-MHSP are compared with that of R-MHSP and GEM. The F-R-MHSP permits good electron collection and efficient blocking of ions, both originated from the first element itself and that from avalanches in successive cascade elements. The IBF reduction in cascaded gaseous micro-hole multipliers incorporating first-element F-R-MHSPs is demonstrated and discussed in view of their potential applications in tracking devices and GPMs.

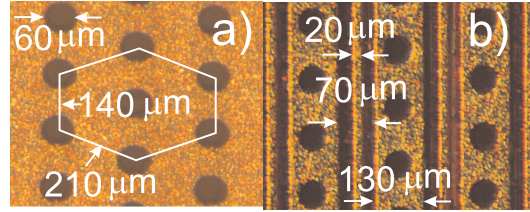


Figure 1. A two-sided microscope photograph of a MHSP electrode with $20\mu\text{m}$ anode strips and $130\mu\text{m}$ cathode strips.

2. The F-R-MHSP concept

In the R-MHSP (figure 2a), a MHSP electrode is mounted with its strips facing the next multiplying element; the bias scheme on the strips is reversed compared to the MHSP, namely the narrow strips are biased negatively compared to the wide strips encompassing the holes. Electrons collected into the holes induce charge multiplication within the holes; unlike the MHSP, there is no further charge multiplication on the strips.

The negatively charged strips trap ions originated from successive multiplying elements. However, like in a GEM, avalanche-ions created within the R-MHSP holes remain uncollected and reach the drift volume (or the PC). The idea of flipping the R-MHSP with its patterned strips pointing towards the drift volume (or the PC), aims at collecting all back-drifting ions, including those originating from its own hole-avalanches. The flipped R-MHSP (F-R-MHSP) is shown schematically in figure 2b. Like in the R-MHSP mode, the narrow ion-collection strips (figure 1) are biased more negative than the broader ones; the multiplication occurs only within the holes. The F-R-MHSP can be inserted anywhere along the cascaded multiplier, but its best performance is expected when used as the first multiplying element.

3. Methodology.

The MHSP and GEM electrodes employed in this work, of $28\times 28\text{mm}^2$ effective area, were produced at the CERN printed circuit workshop, from $50\mu\text{m}$ thick Kapton foil with $5\mu\text{m}$ copper cladding on both sides. The etched double-conical $70/50\mu\text{m}$ (outer/inner) diameter GEM holes are arranged in hexagonal pattern of pitch $140\mu\text{m}$. The MHSP pattern and dimensions are shown in figure 1. All electrodes were stretched onto small G-10 frames. The semitransparent PC was

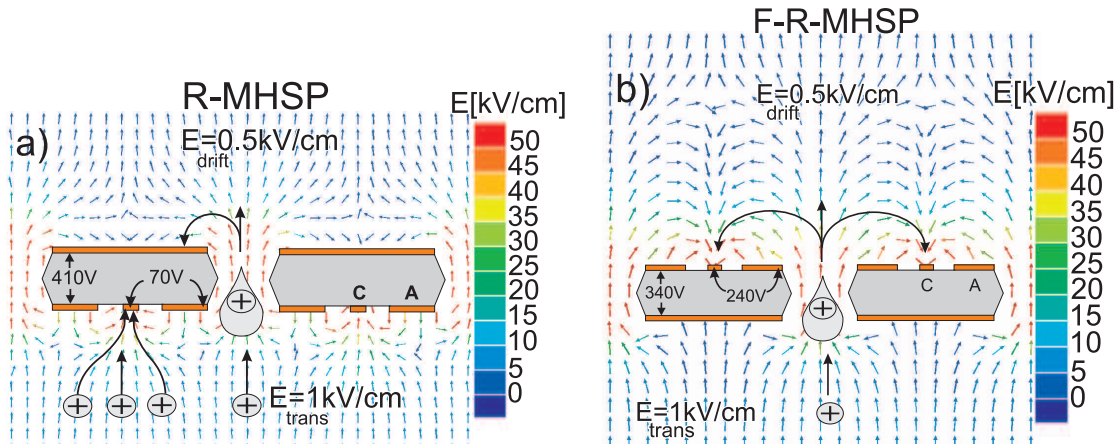


Figure 2. The electric-field vectorial maps calculated by MAXWELL software package [9] in the vicinity of the electrodes and schematic views of the operation principles for: a) reversed-biased R-MHSP and b) flipped reversed biased F-R-MHSP. The potentials selected for the field-map calculations and the color code of the fields are shown in the figures.

5mm in diameter; it was made of 300Å thick layer of CsI, evaporated on a UV transparent window, pre-coated with a 40Å thick Cr film.

The detector elements were mounted within a stainless-steel vessel evacuated with a turbo-molecular pump to 10^{-5} Torr prior to gas filling. The detector was operated with Ar/CH₄ (95/5) at 760 Torr, under regulated gas flow. It was irradiated with a continuous Ar(Hg) UV-lamp through the window. Each of its electrodes was biased independently with a CAEN N471A or CAEN N126 power supply.

In all multiplier-cascade configurations, the currents on biased electrodes were recorded as a voltage-drop on a 40MΩ resistor with a Fluke 175 voltmeter of 10MΩ internal impedance. Their combined resistance was 8MΩ from which the anode current was calculated. The final avalanche-induced currents following charge multiplication were always kept well below 100 nA by attenuating the UV-lamp photon flux with absorbers, if necessary, to avoid charging-up effects. The currents on grounded electrodes were recorded with a Keithley 485 picoamperemeter.

4. Experimental studies and results.

4.1 Single-electron detection efficiency of R-MHSP and F-R-MHSP

In cascaded gaseous hole-multipliers (e.g a R-MHSP, a F-R-MHSP or simply a GEM), to reach full detection efficiency of single photoelectrons emitted from a photocathode, or of ionization electrons radiation-induced within the drift volume, two conditions have to be fulfilled:

- The electron's collection efficiency into holes, particularly in the application to single-photon GPMs, has to be close to unity; this was indeed confirmed for GEMs [10, 11] and more recently for MHSPs (see below), which have slightly more "opaque" hole geometry (figure 1);

- The visible gain (defined as the number of electrons, per single initial electron, transferred from a given multiplier element into a consecutive electrode [1]), of the first element in the cascade should be large enough to ensure full efficiency of the event's detection by the following elements.

These two conditions are of prime importance, because an electron lost at the first multiplication element due to inefficient focusing, insufficient multiplication or inefficient extraction and transfer into the next multiplication stage, cannot be recovered. Indeed, it was found that the R-MHSP biasing scheme reduces the extraction efficiency of the avalanche electrons from the holes towards the next element in the cascade, thus reducing the visible gain of this multiplier [1]. In the F-R-MHSP the strips are facing the PC and could affect photoelectron focusing into the holes; therefore, the focusing efficiency has to be carefully determined.

The photon detection efficiency in GPMs, ε_{photon} , depends on both: the PC's quantum efficiency (QE) and on the single-photoelectron detection efficiency ε_{det} ; it is defined as:

$$\varepsilon_{photon} = QE \cdot \varepsilon_{det}. \quad (4.1)$$

ε_{det} depends on many parameters: the detector geometry, the gas mixture, the electric field conditions, the multiplier gain, the electronics system etc. Once emitted from the photocathode surface into the gas, the photoelectron has to be focused into the first amplifying stage of the detector, namely into the holes. The mechanism of electron extraction, transfer and multiplication in cascaded GEMs for hole voltage values exceeding 320V were extensively studied in [11].

While the operation properties of the MHSP were well established [12], those of the R-MHSP, F-R-MHSP and GEM operating at hole voltages lower than 320V required some more basic study. The studies of single-electron detection efficiency for the R-MHSP and the F-R-MHSP were designed to yield better understanding of the role of the various potentials and of the conditions for reaching minimal IBF values while keeping minimal electron losses.

The parameters affecting the R-MHSP and F-R-MHSP operation are:

1. the hole voltage (V_{hole}); it controls the multiplication and the IBF values of the first multiplying element;
2. the anode-to-cathode strip voltage (ΔV_{AC}); it reduces the visible gain of a single R-MHSP; it could affect the focusing properties of the F-R-MHSP and reduce the IBF from successive elements and from its own avalanches;
3. the transfer field below the R-MHSP or the F-R-MHSP (E_{trans} in figure 2a and figure 2b); it could, in principle, affect both the IBF from successive elements and the visible gain of the R-MHSP or the F-R-MHSP;

It should be noted that except second condition, similar remarks also apply to a GEM.

If we take a GPM as example, the possible fate of the photoelectron after its emission from the photocathode is schematically shown in figure 3.

The single-photoelectron detection efficiency can thus be described as:

$$\epsilon_{det} = \epsilon_{extr} \cdot \epsilon_{hole} \cdot \epsilon_{trans} \quad (4.2)$$

Here ϵ_{det} is the probability to detect a single photoelectron, ϵ_{extr} is the probability to extract a photoelectron from the PC, ϵ_{hole} is the probability to get this electron into the hole and ϵ_{trans} is the probability to transfer an avalanche electron to the next multiplication stage.

As mentioned above, all the measurements were performed in Ar/CH₄(95/5) under atmospheric pressure. In all the measurements presented below we assumed $\epsilon_{extr} = 1$ in equation (4.2). Realistic ϵ_{extr} values are well known, and were previously measured as function of the drift field above a photocathode for a variety of gas mixtures [13]. Thus the measured electron detection efficiency in TPC or GPM conditions (low or high drift fields) can be straightforwardly corrected, using the known ϵ_{extr} at the corresponding drift field and gas mixture. For instance, in atmospheric Ar/CH₄ (95/5) used in all our measurements, $\epsilon_{extr}=70\%$ at drift fields of 0.5kV/cm. In TPC conditions, there is no PC and the parameter ϵ_{extr} is not relevant; therefore, equation (4.2) with $\epsilon_{extr}=1$ is exact.

Due to the statistical fluctuations in the amplification process of single electrons, many events have only a small number of electrons at the exit of the holes of the first amplifying element. DC measurements (e.g. ratio of the current after multiplication to that of primary photoelectrons) are not sensitive to single-photoelectron losses or to events with small gain; their contribution to the total current is negligible when the detector is operated in multiplication mode. Under these conditions, the only way to assess the single-electron detection efficiency ϵ_{det} , is by event pulse-counting. Current-mode measurements provide valid results for single-photoelectron transport, only if the detector is operated at unity gain. In these conditions, currents measured on the detector's electrodes are due to the transfer of the primary photoelectrons only - which is not a subject of our studies. A more detailed discussion on this subject can be found in [14].

We found it convenient to measure ϵ_{det} of the hole multipliers by comparing their event-rate to the one measured with a multi-wire proportional counter (MWPC) - known to have $\epsilon_{det}=1$ [11, 15, 16]. This strategy has been used in many of our previous studies, and was discussed in detail [11, 15, 16]. figure 4a shows the dedicated experimental setup. It consists of a UV-transparent quartz (Suprasil) window with CsI semitransparent PCs evaporated on both surfaces, sandwiched between the reference MWPC detector and the investigated multiplier (R-MHSP/MWPC, F-R-MHSP/MWPC or GEM/MWPC). Both, reference and investigated detectors operate at equal total gains; the MWPC following each investigated hole-multiplier was added to keep the total gain high enough for pulse counting. The ratio of the number of detected events, with equal electronic thresholds, multiplied by the ratio of initial photocurrents of the top-face and bottom-face PCs, provided the absolute single-electron detection efficiency of the GEM, the R-MHSP and the F-R-MHSP multipliers. This experimental technique relies on precise measurements of the exponential pulse-height distributions of the multiplied single electrons, needed for adjusting equal conditions in both the reference MWPC and the investigated hole-multiplier/MWPC elements. This method can be naturally applied only in proportional-mode operation; it is no longer applicable in conditions of charge saturation or with feedback effects - leading to spectra that deviate significantly from the exponential. A more detailed explanation on this method can be found elsewhere [15, 16].

Measurements with R-MHSP. The photoelectron detection efficiency of the R-MHSP as

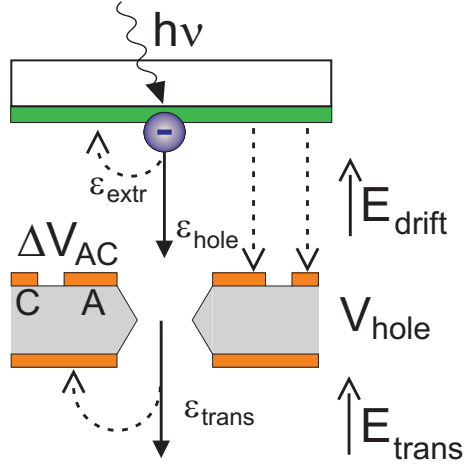


Figure 3. Electron transfer through a F-R-MHSP. Photoelectrons emitted from a PC are extracted from the photocathode with an efficiency ϵ_{extr} , guided into the apertures of the F-R-MHSP with an efficiency ϵ_{hole} . A fraction of the avalanche electrons is extracted and transferred into a following element with an efficiency ϵ_{trans} ; another fraction is lost to the bottom electrode. The electron transfer through either a GEM or a R-MHSP is described the same way, the F-R-MHSP was taken as an example.

function of the inter-strip voltage (potential difference between the anode and cathode strips) ΔV_{AC} is presented in figure 5 for typical "TPC conditions" (i.e. $E_{drift}=0.2\text{kV/cm}$) and for "GPM conditions" (i.e. $E_{drift}=0.5\text{kV/cm}$). In GPM conditions, the measurements were performed at V_{hole} values of 360V, 380V and 400V; in TPC conditions, at 360V and 380V. In all cases, the transfer field was set to 1kV/cm. The visible gains as a function of the inter-strip voltage are also presented for each set of measurements. The visible gain G_{VIS} is derived from the ratio of the current I_M measured at the interconnected electrodes of bottom MWPC (see figure 4b), to the PC photocurrent I_{PC0} , measured in photoelectron collection mode (no gain):

$$G_{VIS} = \frac{I_M}{I_{PC0}}. \quad (4.3)$$

From figure 5 we learn that:

1. Both the visible gain and the photoelectron detection efficiency are only slightly affected by the drift field. The reason is probably that the field inside the holes is not affected by the drift field (within the present conditions).
2. Although it is desirable to increase ΔV_{AC} , as to divert more ions towards the cathode strips, the drop in the visible gain (figure 5), and consequently in the detection efficiency, sets a limit to this parameter. ΔV_{AC} can be raised if the loss of electrons is compensated by a further increase of V_{hole} . For each hole-voltage, the maximal strip voltage could be found at which the photoelectron detection efficiency is close to unity. The maximal strip voltages at which the detection efficiency is $\sim 100\%$ are 60V, 70V and 90V at corresponding hole voltages of 360V, 380V and 400V. These inter-strip voltages correspond to a visible gain of about 20 on the R-MHSP as can be seen in figure 5.

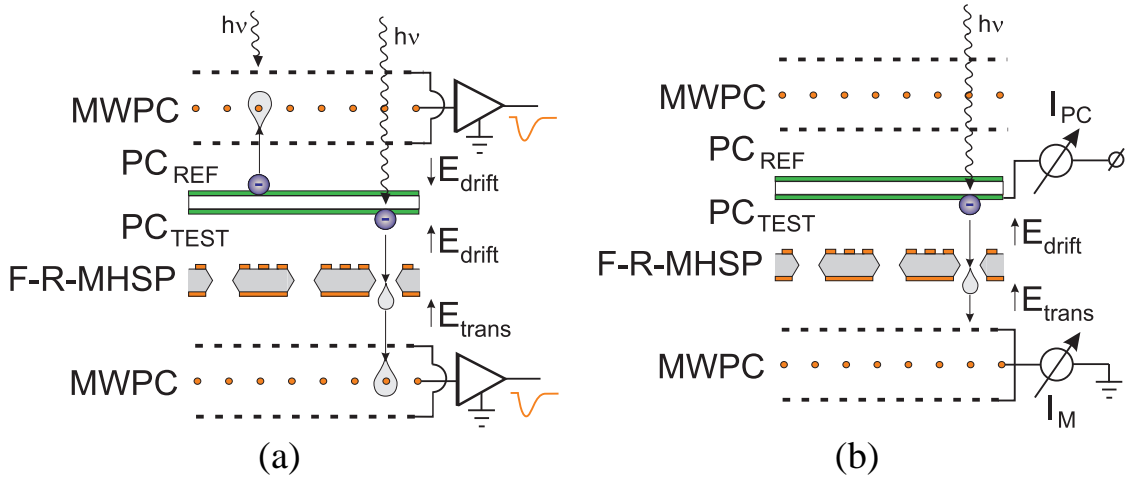


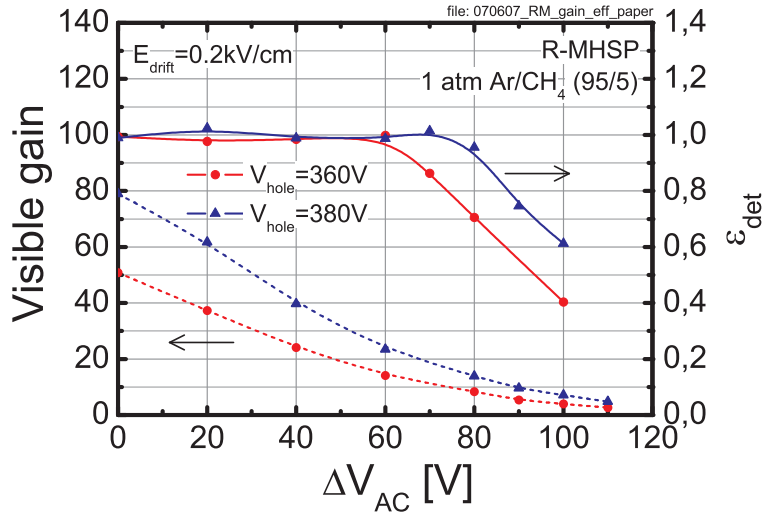
Figure 4. The schematic view of the experimental setup for measuring the single-electron detection efficiency of a F-R-MHSP (a) and its visible gain (b). Similar setups were used for measuring the same properties of a R-MHSP and a GEM

Measurements with F-R-MHSP Measurements similar to that of the R-MHSP were performed for the F-R-MHSP. As mentioned above, in the F-R-MHSP configuration, the strips are facing towards the drift region or to the PC. Therefore, the electron transfer to the next amplification stage is expected to be unaffected by varying the strip voltage. However, the increase of the inter-strip voltage difference could, in principle, affect focusing of photo-electrons into the holes of the F-R-MHSP itself. As in the case of the R-MHSP, here too we need to optimize the strip-and-hole-voltages. The inter-strip voltage has to be large enough for better ion collection, while the hole-voltage has to be low enough for reaching lower IBF values in this element; in addition, the condition of photoelectron detection efficiency close to unity has to be fulfilled.

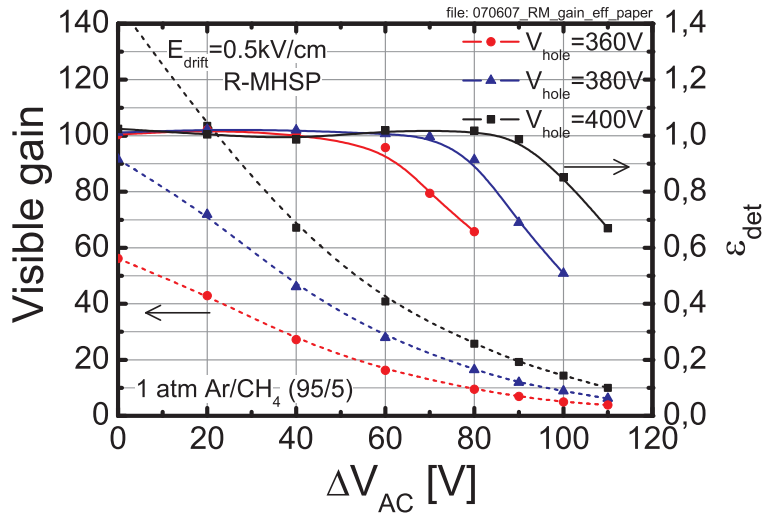
In our setup, the transfer field was set to 1kV/cm. In figure 6, the photoelectron detection efficiency of the F-R-MHSP is shown for TPC conditions ($E_{drift}=0.2$ kV/cm) and for GPM conditions ($E_{drift}=0.5$ kV/cm). In each regime, the measurements were performed at different hole voltages of 310V, 320V, 340V and 360V.

We can see in figure 6 that:

1. The visible gain of the F-R-MHSP does not depend on variations in the inter-strip voltage. This can be considered as a first indication of a good focusing of photoelectrons into the holes (independent on the inter-strip voltage).
2. The photoelectron detection efficiency is low for small inter-strip voltages. This can be attributed to a partial collection of photoelectrons by the narrow anode strips. As we increase the inter-strip voltage, the efficiency is rising up, reaching a plateau.
3. The minimal hole-voltage which provides close to full photoelectron detection efficiency was measured to be 320V. It corresponds to a visible gain of ~ 10 (figure 6).



(a)



(b)

Figure 5. The visible gain (left y-axis, dashed lines) and the photoelectron detection efficiency (right y-axis, solid lines) as a function of the inter-strip voltage ΔV_{AC} of a R-MHSP in TPC conditions ($E_{drift}=0.2\text{kV/cm}$) (a) and GPM conditions ($E_{drift}=0.5\text{kV/cm}$) (b). Measurements performed at different values of hole voltage.

In some conditions the single electron pulse height spectrum deviates from a pure exponential, leading to an error in normalization. This is the case for the data points in figure 6a, $V_{hole}=360\text{V}$ and $\Delta V_{AC}<80\text{V}$, where a Polya distribution was observed, leading to overestimated efficiency values.

Measurements with GEM As we mentioned above, the photoelectron detection efficiency of the GEM was not yet measured at a hole voltage lower than 320V [11]. The detection efficiency of a single GEM as a function of its visible gain is presented in figure 7. During measurements, the transfer field between the GEM and the MWPC was kept at 1kV/cm. It was found that the minimal hole voltage which permits the operation of the GEM at full detection efficiency for single electrons is around 280V. That corresponds to a visible gain of ~ 10 on the GEM.

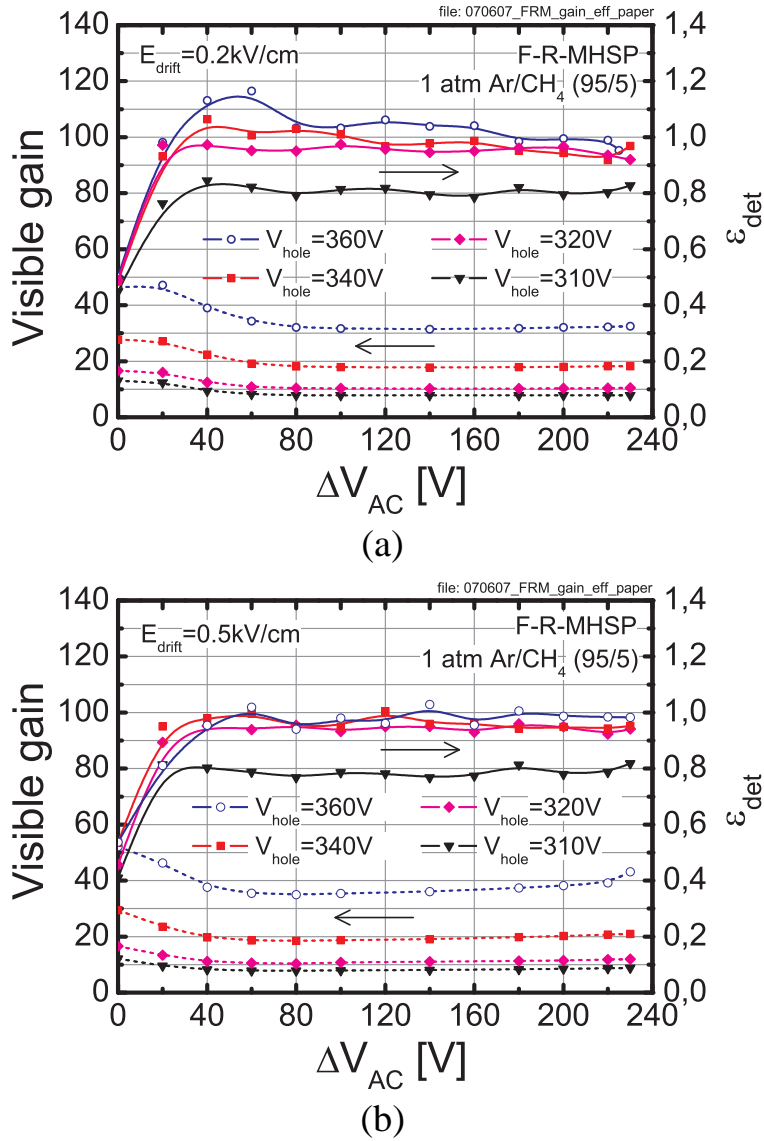


Figure 6. The visible gain (left y-axis, dashed lines) and the photoelectron detection efficiency (right y-axis, solid lines) as a function of the inter-strip voltage of a F-R-MHSP in TPC conditions ($E_{drift}=0.2\text{kV/cm}$) (a) and GPM conditions ($E_{drift}=0.5\text{kV/cm}$) (b). Measurements performed at different values of hole voltage.

4.2 Studies of ion blocking capability of the first element in a cascade

The IBF reduction capability of the first element was studied in a setup depicted in figure 8 with a first element being a GEM, a R-MHSP or a F-R-MHSP. It was followed by a GEM, of which the avalanche acts as a source of back-flowing ions. This second GEM element was biased at 420V (gain ~ 2000); the transfer field in the gap between the two elements was $E_{trans}=1\text{kV/cm}$ and the drift field was $E_{drift}=0.5\text{kV/cm}$ (GPM conditions) (figure 9a) and 0.2kV/cm (TPC conditions) (figure 9b).

The total avalanche current in this configuration was measured as the sum of currents from the

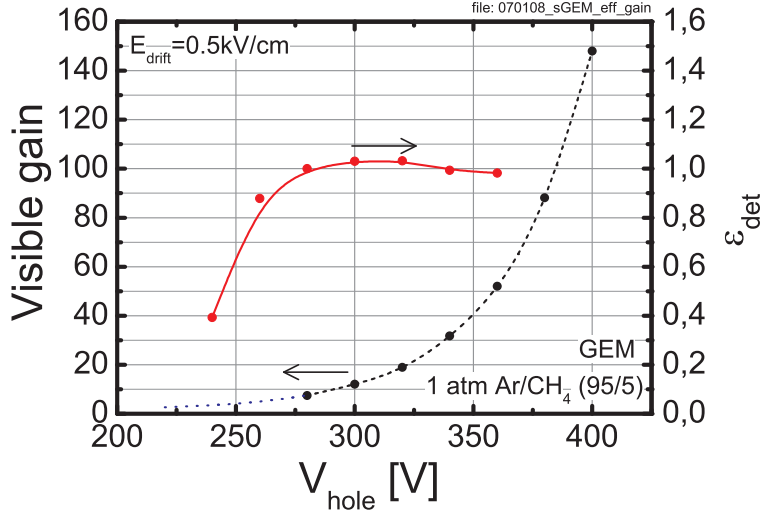


Figure 7. The visible gain (left y-axis, dashed line) and the photoelectron detection efficiency (right y-axis, solid line) as a function of the hole voltage of the GEM in GPM conditions ($E_{drift} = 0.5 \text{ kV/cm}$). For voltages below 280V (dotted line), the gain curve was extrapolated with an exponential function (dotted line).

bottom anode and the bottom GEM electrode (as shown in figure 8). The IBF was calculated as the ratio of the PC avalanche current I_{APC} (under avalanche multiplication), to the total avalanche current I_A :

$$\text{IBF} = \frac{I_{APC}}{I_A} \quad (4.4)$$

Where the PC avalanche current I_{APC} was calculated as a difference of the total PC current under multiplication I_{TOTPC} and the initial I_{0PC} PC current: $I_{APC} = I_{TOTPC} - I_{0PC}$.

The correlation between the IBF and the total gain (of both elements) measured in these conditions is presented in figure 9. The parameters (fixed and variable) in these measurements were the following:

- R-MHSP: the inter-strips voltage (ΔV_{AC}) varied from 0V to 60V and the hole voltage was set to 360V (following the results of previous section);
- F-R-MHSP: the inter-strips voltage (ΔV_{AC}) varied from 0V to 230V and the hole voltage was set to 320V (following results of the previous section);
- GEM, the hole voltage (V_{hole}) was varied in the range 280V-340V.

In TPC conditions, the R-MHSP and the F-R-MHSP followed by a GEM performed 3 and 6 times better, respectively, than the double-GEM in terms of IBF reduction at a total gain of $\sim 1.2 \cdot 10^4$. The IBF values of all three multipliers improved at the lower drift field; e.g., that of the F-R-MHSP reached the value of 0.005.

One can note that in GPM conditions, the IBF measured with either the R-MHSP/GEM or the F-R-MHSP/GEM is 4-fold lower compared to that of a double-GEM, at a gain of $\sim 1.5 \cdot 10^4$ (figure

9). In these conditions, both the R-MHSP and the F-R-MHSP provided practically the same IBF values, of about 0.015.

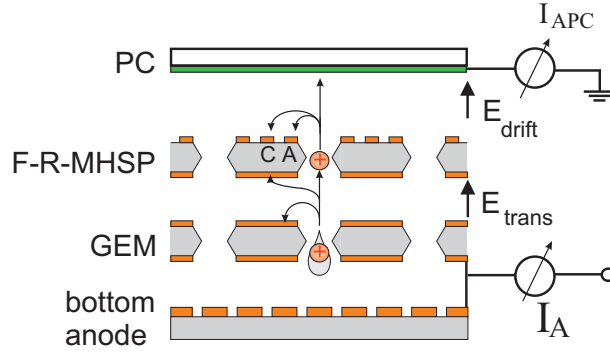


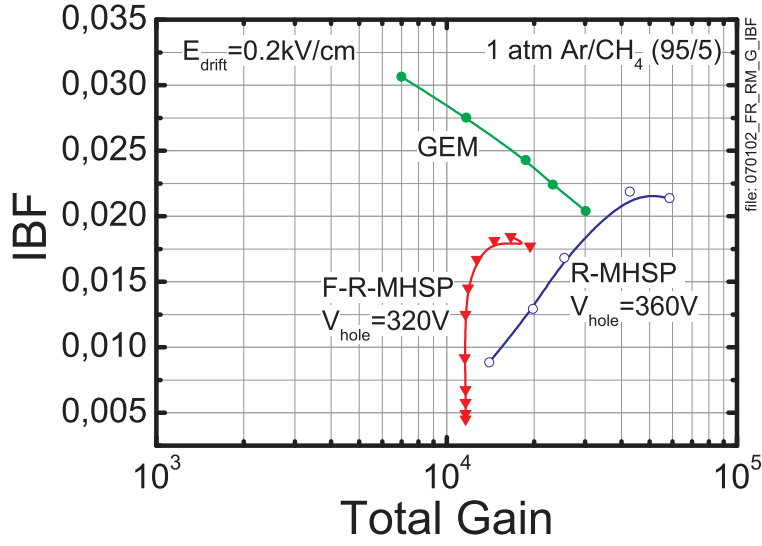
Figure 8. The schematic view of the setup for measurements of ion blocking capability of the F-R-MHSP. Here the GEM serves as a source of avalanche ions. The avalanche charge was collected at the interconnected GEM-bottom and bottom anode electrodes. Similar measurements were performed with R-MHSP and GEM elements followed by a GEM.

4.3 IBF in cascaded multipliers incorporating R-MHSP, F-R-MHSP, GEM and MHSP elements.

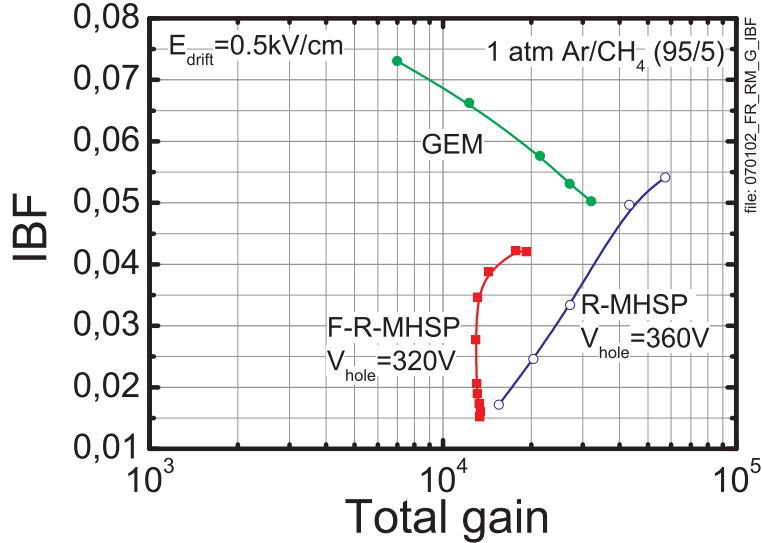
Systematic investigations were carried out in two types of cascades multipliers: the R-MHSP/GEM/MHSP (figure 10a) and F-R-MHSP/GEM/MHSP (figure 10b). The last MHSP element in each configuration was chosen based on its known 5-fold IBF reduction compared to a GEM [12], in addition to that of the two types of first-element multipliers investigated here. The optimized transfer- and induction-field configurations suggested in [12, 17] were combined with the insight from the F-R-MHSP and R-MHSP studies described above. The measurements were performed both in TPC conditions ($E_{drift}=0.2\text{kV/cm}$) and GPM conditions ($E_{drift}=0.5\text{kV/cm}$). The following parameters were chosen (see figure 10): $E_{trans1}=1\text{kV/cm}$; $E_{trans2}=60\text{V/cm}$ (following [17]) and $E_{ind}=-5\text{kV/cm}$; the latter "reversed" field, permitted collecting most of the last-avalanche ions at the bottom mesh cathode (following [12]). The voltages across the holes and between strips for different elements were the following: The first-element voltages were chosen according to the results described above: $V_{hole1}=320\text{V}$; $\Delta V_{AC1}=230\text{V}$ for the F-R-MHSP and $V_{hole1}=360\text{V}$; $\Delta V_{AC1}=60\text{V}$ for the R-MHSP. The GEM and MHSP potentials were chosen as follows:

- In TPC conditions, for the F-R-MHSP/GEM/MHSP detector: $V_{GEM1}=230\text{V}$; for the R-MHSP/GEM/MHSP detector: $V_{GEM1}=240\text{V}$.
- In GPM conditions, we had to increase the GEM voltage and further optimize the second transfer field. For the F-R-MHSP/GEM/MHSP: $V_{GEM1}=275\text{V}$, $E_{trans2}=75\text{V/cm}$; for the R-MHSP/GEM/MHSP: $V_{GEM1}=300\text{V}$, $E_{trans2}=100\text{V/cm}$.

The last-element MHSP multiplier was polarized, in both setups, as follows: $V_{hole2}=370\text{V}$ and ΔV_{AC2} was varied between 140V and 230V, to adjust the total gain of the whole cascaded detector.



(a)



(b)

Figure 9. The IBF and total gain measured in the setup of figure 8 with R-MHSP/GEM, F-R-MHSP/GEM and 2GEM configurations, at TPC (a) and GPM (b) conditions. In the case of R-MHSP/GEM and F-R-MHSP/GEM the gain was varied by changing the inter-strip voltage from 0V to 60V and from 0V to 230V correspondingly; in the case of 2GEMs - by changing the hole voltage from 280V to 340V. The hole voltages of the R-MHSP and F-R-MHSP were fixed at the values indicated in the figure, to ensure full photoelectron detection efficiency.

The IBF is presented in correlation with the total gain, for drift-field values of 0.2kV/cm (figure 11a) and 0.5kV/cm (figure 11b).

The IBF recorded at a total gain of $\sim 10^4$ in the TPC operation mode (drift field of 0.2kV/cm) was $\sim 1.5 \cdot 10^{-4}$ with a F-R-MHSP first-element multiplier; it was $\sim 8 \cdot 10^{-4}$ with a R-MHSP first

element. In these conditions, the respective numbers of ions back-flowing into the drift region are: ~ 1.5 and ~ 8 ions per primary ionization electron.

In the GPM operation mode, the lowest IBF value reached was $3 \cdot 10^{-4}$ for the F-R-MHSP/GEM/MHSP and $9 \cdot 10^{-4}$ for R-MHSP/GEM/MHSP, at a detector total gain of $\sim 10^5$. It means that per single-photon event, on the average, 30 or 90 ions reach the PC in a cascaded detector with a F-R-MHSP or a R-MHSP first-element multiplier, correspondingly.

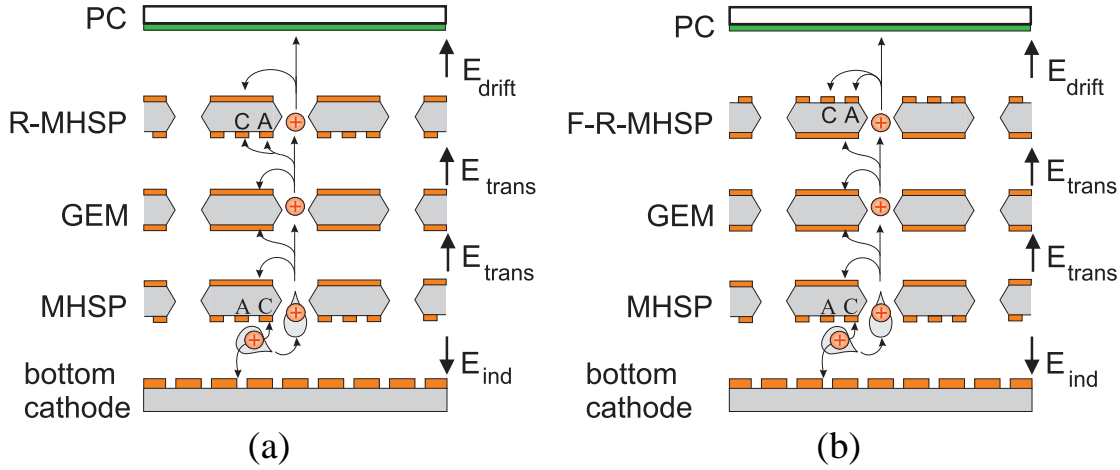


Figure 10. Schemes of cascaded R-MHSP/GEM/MHSP (a) and F-R-MHSP/GEM/MHSP (b) multipliers coupled to a semi-transparent photocathode; possible avalanche ions paths are also shown.

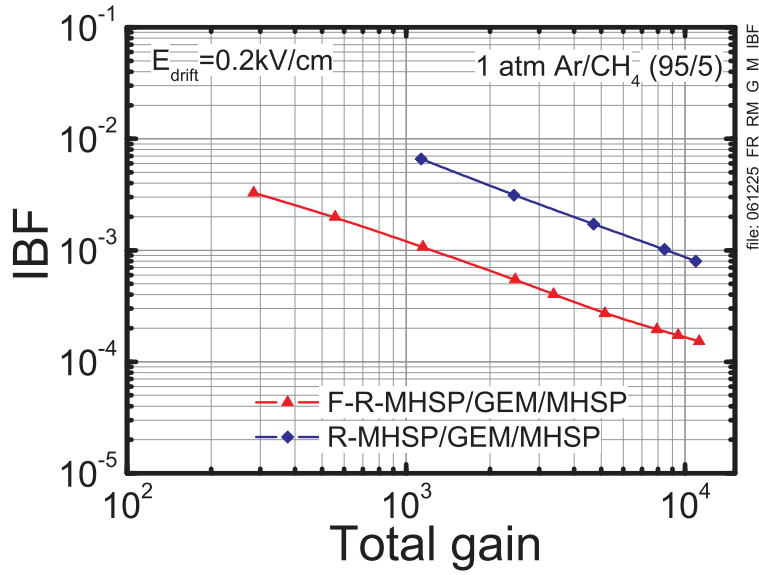
5. General discussion

In this work we have continued our long ongoing studies of IBF reduction in cascaded electron multipliers, searching for further improvements that will permit more stable gaseous detector operation.

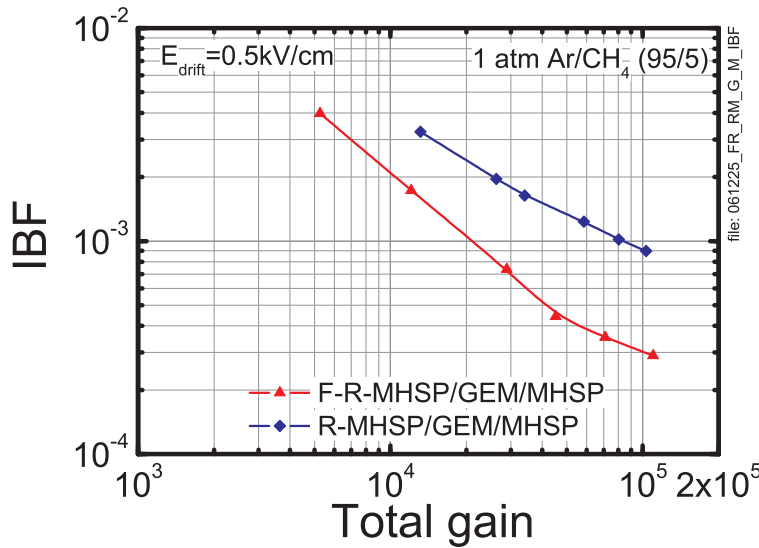
Following the 5-fold and the additional 3-fold IBF reduction (compared to GEM) with MHSP and R-MHSP, respectively, we investigated here a third operation mode of the MHSP element: the "flipped Reversed-bias Micro-Hole & Strip Plate" (F-R-MHSP). Unlike in MHSP and the R-MHSP, in the F-R-MHSP mode the strips are facing towards the drift region. This operation mode permits uniquely capturing both: ions originated from the first multiplier and that induced by the avalanches of the successive cascade elements. The F-R-MHSP is therefore best suitable as the first element of a cascaded multiplier.

A systematic comparative study of the F-R-MHSP, R-MHSP and GEM elements yielded operation conditions with full collection efficiency of primary electrons into the multiplying holes and the efficient avalanche-electrons transfer into the following elements of a cascade. Conditions were found in which the inter-strip potentials in the F-R-MHSP and R-MHSP were optimized for both: electron collection and ion blocking.

It was found that for R-MHSP at hole voltages of 360V, 380V and 400V, the inter-strip potential can be raised to 60V, 70V and 90V correspondingly, maintaining full single-electron detection



(a)



(b)

Figure 11. The IBF in correlation with the total gain of the R-MHSP/GEM/MHSP (figure 10a) and F-R-MHSP/GEM/MHSP (figure 10b) cascaded detectors, with semitransparent photocathodes; the IBF is plotted for drift fields of 0.2kV/cm (TPC conditions) (a) and 0.5kV/cm (GPM conditions) (b).

efficiency. This was measured at a fixed transfer field of 1kV/cm. Further increase of the transfer field will allow further increase of the inter-strip voltages; this will allow to divert more ions to the cathode strips, with no sacrifice to the photoelectron detection efficiency [1].

Field distortions in the drift region, at the hole vicinity, due to the applied F-R-MHSP inter-strip voltage, did not affect the electron focusing into the hole apertures under the current operation conditions (figure 6). This is due to the very intense focusing field in the hole vicinity which is

effectively focusing the drifting electrons. It should be mentioned that, the drift field is not uniform within a small region of few hundred microns above the F-R-MHSP's top surface (figure 2b), in which the back-flowing ions are trapped. The main limitation on the detection efficiency of the F-R-MHSP arises from insufficient multiplication within the holes; full detection efficiency, in the present operation conditions, was reached for hole voltages exceeding 320V at a transfer fields of 1kV/cm.

Theoretical calculations of the minimal visible gain required for close-to-full single-photoelectron detection efficiency with R-MHSP, performed in [1], were partly confirmed by the present experimental data. It was calculated in [1] that a visible gain of 25 for the R-MHSP implies that, with an exponential single-electron pulse-height distribution, in 92% of the events at least two electrons are transferred to the following element in the cascade. Indeed, the present experimental measurements showed that a single photoelectron is detected with $\sim 100\%$ efficiency at a visible gain close to 20 (figure 5 and figure 6). Experimentally, we found single-electron detection efficiency $>90\%$ already at a visible gain of about 10 and close to 100% at a visible gain of 20 and above (figure 5 and figure 6).

The ion blocking capability was studied in cascaded detector configurations where a GEM, R-MHSP or F-R-MHSP was used as the first element, followed by a GEM; the latter served as the source of avalanche ions.

In TPC conditions, a 3-fold lower IBF was reached with a R-MHSP compared to that with a first-element GEM; the F-R-MHSP yielded a 6-fold better ion blocking compared to GEM.

In GPM conditions, the experiment showed 4-fold lower IBF with either first-element R-MHSP or F-R-MHSP, compared with that of a standard GEM. It should be noted however that it was not possible to maintain both high gain (above 10^4) and low IBF in "GPM conditions", for the detector comprised of only two multiplication stages. Naturally, additional elements could be added to the cascade to provide higher total gains.

In the F-R-MHSP/GEM/MHSP detector with a semitransparent PC, the IBF value reached in a GPM mode ($E_{drift}=0.5\text{kV/cm}$), compatible with full single-electron detection efficiency, was $3 \cdot 10^{-4}$ at a total gain of $\sim 10^5$. This record IBF value seems to be sufficient for a stable operation of the multiplier in combination with a visible-light sensitive photocathode (e.g. bialkali). With the resulting 30 ions impinging on the photocathode per single-photoelectron event, a bialkali PC will induce on the average 0.6 secondary electrons (calculated according to [14]). This could be a significant step forward in the field of GPMs; it will permit, on one hand, a stable DC operation of a detector with single-photon sensitivity in the visible spectral range and on the other hand will drastically reduce the photocathode aging [4]. However, one should keep in mind that the number of secondary electrons can fluctuate, due to fluctuations of the number of electrons in individual avalanches; therefore there could be more than one secondary electron per avalanche. This phenomenon is well understood for low-pressure gases setting the condition for breakdown. The breakdown does not occur as far as the average number of secondary electrons liberated from the PC by the back-flowing avalanche ions is below one [18]. At high pressures this condition could not always be applicable, because of possible space charge formation [19] at the PC vicinity. It is probable, however, that at low IBF values, the space charge formation will be prevented and the above mentioned condition for breakdown will be held.

The operation of cascaded visible-sensitive GPMs is currently under investigation, with bial-

kali photocathodes coupled to F-R-MHSP/GEM/MHSP multipliers that provided the lowest IBF values.

The IBF value of $\sim 1.5 \cdot 10^{-4}$ measured in TPC conditions ($E_{drift}=0.2\text{kV/cm}$) at a gain of 10^4 is also the lowest value ever achieved. It is ~ 30 fold lower than the $5 \cdot 10^{-3}$ value recorded in a 3GEM TPC element at a similar gain [17, 20, 8]. In our lower drift-field TPC conditions, much less ions flow back to the drift region; indeed, the IBF decreases linearly with the drift field [21]. With a first-element F-R-MHSP less than 2 ions per avalanche electron return on the average to the drift region; with a first-element R-MHSP, 8 ions flow back to the drift region.

These very low numbers could be of prime importance for the conception of TPC detectors operating in DC mode, with large particle multiplicities at high repetition rates.

Further reduction of the IBF could be reached naturally with additional patterned hole multipliers in the cascade. We are presently investigating the idea of double-face patterned hole-multipliers, with ion-defocusing strips running on both faces

Acknowledgments

This work is partly supported by the Israel Science Foundation, grant No 402/05, by the MINERVA Foundation and by Project POCTI/FP/63441/2005 through FEDER and FCT (Lisbon). A. Breskin is the W.P. Reuther Professor of Research in The Peaceful Use of Atomic Energy.

References

- [1] A. Lyashenko et al., *Advances in ion back-flow reduction in cascaded gaseous electron multipliers incorporating R-MHSP elements*, *JINST* **1** (2006) P10004. [physics/0606210]
- [2] J. F. C. A. Veloso et al., *A proposed new microstructure for gas radiation detectors: The microhole and strip plate*, *Rev. Sci. Instr. A* **71** (2000) 2371.
- [3] D. Mormann et al., *Evaluation and reduction of ion back-flow in multi-GEM detectors*, *Nucl. Instr. and Meth. A* **516** (2004) 315.
- [4] A. Breskin et al., *Ion-induced effects in GEM and GEM/MHSP gaseous photomultipliers for the UV and the visible spectral range*, *Nucl. Instr. and Meth. A* **553** (2005) 46 and references therein. [physics/0502132]
- [5] J. F. C. A. Veloso et al., *The Photon-Assisted Cascaded Electron Multiplier: a concept for potential avalanche-ion blocking*, *JINST* **1** (2006) P08003. [physics/0606209]
- [6] A. Buzulutskov et al., *Electric and Photoelectric Gates for ion backflow suppression in multi-GEM structures*, *JINST* **1** (2006) P08006.
- [7] J. F. C. A. Veloso et al., *MHSP in reversed-bias operation mode for ion blocking in gas-avalanche multipliers*, *Nucl. Instr. and Meth. A* **548** (2005) 375. [physics/0503237]
- [8] S. Roth et al., *Charge transfer of GEM structures in high magnetic fields*, *Nucl. Instr. and Meth. A* **535** (2004) 330.
- [9] *MAXWELL Commercial Finite Element Computation Package*, Ansoft Co. Pittsburg, PA, USA.
- [10] S. Bachmann et al., *Charge amplification and transfer processes in the gas electron multiplier*, *Nucl. Instr. and Meth. A* **438** (1999) 376.

- [11] C. Richter et al., *On the efficient electron transfer through GEM*, *Nucl. Instr. and Meth. A* **478** (2002) 538.
- [12] J.M. Maia et al., *Avalanche-ion back-flow reduction in gaseous electron multipliers based on GEM/MHSP*, *Nucl. Instr. and Meth. A* **523** (2004) 334.
- [13] A. Buzulutskov et al., *The GEM photomultiplier operated with noble gas mixtures*, *Nucl. Instr. and Meth. A* **443** (2000) 164 and references therein.
- [14] D. Mörmann, *Study of novel gaseous photomultipliers for UV and visible light*, Ph.D. thesis, Weizmann Institute of Science, Israel., *JINST TH 004* (2005)
- [15] D. Mörmann et al., *Operation principles and properties of the multi-GEM gaseous photomultiplier with reflective photocathode*, *Nucl. Instr. and Meth. A* **530** (2004) 258.
- [16] C. Shalem et al., *Advances in thick GEM-like gaseous electron multipliers. Part 1: atmospheric pressure operation*, *Nucl. Instr. and Meth. A* **558** (2006) 475.
- [17] M. Killenberg et al., *Charge transfer and charge broadening of gem structures in high magnetic fields*, *Nucl. Instr. and Meth. A* **530** (2004) 251.
- [18] Robert A. Wijsman, *Breakdown Probability of a Low Pressure Gas Discharge*, *Phys. Rev.* **75** (1949) 833.
- [19] L. B. Loeb and J. M. Meek, *The Mechanism of Spark Discharge in Air at Atmospheric Pressure. I*, *J. Appl. Phys.* **11** (1940) 438.
- [20] S. Lotze et al., *Charge Transfer of GEM Structures in High Magnetic Fields*, *Nucl. Phys. B (Proc. Suppl.)* **150** (2006) 155.
- [21] A. Bondar et al., *Study of ion feedback in multi-GEM structures*, *Nucl. Instr. and Meth. A* **496** (2003) 325.